ARTICLE OPEN ACCESS

Early-onset Parkinson disease caused by a mutation in CHCHD2 and mitochondrial dysfunction

Richard G. Lee, BSc (Hons),* Maryam Sedghi, MSc,* Mehri Salari, MD, Anne-Marie J. Shearwood, MSc, Maike Stentenbach, BSc, Ariana Kariminejad, MD, Hayley Goullee, BSc (Hons), Oliver Rackham, PhD, Nigel G. Laing, PhD, Homa Tajsharghi, PhD,§ and Aleksandra Filipovska, PhD§

Correspondence
Dr. Tajsharghi
homa.tajsharghi@his.se
or Dr. Filipovska
aleksandra.filipovska@uwa.edu.au

Neurol Genet 2018;4:e276. doi:10.1212/NXG.0000000000000276

Abstract

Objective

Our goal was to identify the gene(s) associated with an early-onset form of Parkinson disease (PD) and the molecular defects associated with this mutation.

Methods

We combined whole-exome sequencing and functional genomics to identify the genes associated with early-onset PD. We used fluorescence microscopy, cell, and mitochondrial biology measurements to identify the molecular defects resulting from the identified mutation.

Results

Here, we report an association of a homozygous variant in *CHCHD2*, encoding coiled-coil-helix-coiled-coil-helix domain containing protein 2, a mitochondrial protein of unknown function, with an early-onset form of PD in a 26-year-old Caucasian woman. The *CHCHD2* mutation in PD patient fibroblasts causes fragmentation of the mitochondrial reticular morphology and results in reduced oxidative phosphorylation at complex I and complex IV. Although patient cells could maintain a proton motive force, reactive oxygen species production was increased, which correlated with an increased metabolic rate.

Conclusions

Our findings implicate *CHCHD2* in the pathogenesis of recessive early-onset PD, expanding the repertoire of mitochondrial proteins that play a direct role in this disease.

*These authors contributed equally to the study and share first authorship.

§These authors share senior authorship and are co-corresponding authors.

From the Centre for Medical Research (R.G.L., A.-M.J.S., M. Stentenbach, H.G., O.R., N.G.L., H.T., A.F.), University of Western Australia and the Harry Perkins Institute for Medical Research, Nedlands, Western Australia, Australia; Department of Genetics (M. Sedghi), University of Isfahan, Isfahan; Functional Neurosurgery Research Center (M. Salari), Shohada Tajrish Neurosurgical Center of Excellence, Shahid Beheshti University of Medical Sciences, Tehran, Iran; Kariminejad-Najmabadi Pathology and Genetics Center (A.K.), Tehran, Iran; School of Molecular Sciences (O.R., A.F.), The University of Western Australia, Crawley; Department of Diagnostic Genomics (N.G.L.), PathWest, QEII Medical Centre, Nedlands, Western Australia, Australia; and Division Biomedicine and Public Health (H.T.), School of Health and Education, University of Skovde, Sweden.

Funding information and disclosures are provided at the end of the article. Full disclosure form information provided by the authors is available with the full text of this article at Neurology.org/NG.

The Article Processing Charge was funded by the Australian Research Council.

Glossary

BCA = Bicinchoninic acid; **DHE** = dihydroethidium; **ETC** = electron transport chain; **MICOS** = mitochondrial contact site and cristae organizing system; **NGS** = next-generation sequencing; **OXPHOS** = oxidative phosphorylation; **PBS** = phosphate-buffered saline; **PD** = Parkinson disease; **RCR** = respiratory control ratio; **ROS** = reactive oxygen species; **WES** = whole-exome sequencing.

Parkinson disease (PD, MIM168600) is the most common movement disorder of aging and the second-most common neurodegenerative disease, after Alzheimer disease (MIM104300).[1,2] PD has been associated with mutations in multiple genes including *PARK2, PINK1, PARK7, ATP13A2, SCNA, LRRK2, VPS35, EIF4G1, DNAJC13,* and *CHCHD2*.[3–6]

Recent whole-exome sequencing (WES) of Japanese patients with autosomal dominant or sporadic PD identified a heterozygous *CHCHD2* missense change (p.Thr61Ile) in a family with autosomal dominant late-onset PD.[5] Subsequently, the identical variant was identified in a Chinese family with autosomal dominant PD.[6] Additional *CHCHD2* variants, including p.Ala32Thr, p.Pro34Leu, and p.Ile80Val, have been described in 4 western European familial patients with PD.[7] The pathomechanism of the *CHCHD2* variants in these studies is, however, unclear as is the physiologic role of CHCHD2.

Here, we identify a new *CHCHD2* variant in a patient with autosomal recessive early-onset PD and establish the pathogenic mechanism of this variant. We have shown that the mutation results in a fragmented mitochondrial morphology and reduced electron transport chain (ETC) activity.

Methods

Standard protocol approvals, registrations, and patient consents

The study was approved by the ethical standards of the relevant institutional review board, the Ethics Review Committee in the Gothenburg Region (Dn1: 842-14), and the Human Research Ethics Committee of the University of Western Australia. Informed consent was obtained from patients included in this study after appropriate genetic counseling. Blood samples were obtained from patients, their parents, and siblings.

Clinical evaluation

Medical history was obtained, and physical examination was performed as part of routine clinical workup.

Genetic analysis

Next-generation sequencing (NGS) whole-exome and/or targeted neuromuscular panel sequencing (WES or neuromuscular sub-exomic sequencing [NSES]) was performed on the patient's DNA. Confirmatory bidirectional Sanger sequencing was performed in patients with PD and their family members (see e-Methods, links.lww.com/NXG/A85).

Cell culture and transfections

Dermal fibroblast cultures from the patient were established by standard protocols, after written informed consent was obtained. Cultured fibroblasts from a healthy age-matched individual were used as a control. Detailed methods are provided in supplementary information.

Mitochondrial isolation and cell lysis

Mitochondria were isolated from fibroblasts as previously described.[8] Cell lysates were prepared using a buffer containing the following: 150 mM NaCl, 0.1% (vol/vol) Triton X-100, and 50 mM Tris-HCl (pH 8.0). Protein concentration was determined using a bicinchoninic acid (BCA) assay.

Fluorescence microscopy

Detailed methods are described in the supplementary material, links.lww.com/NXG/A85.

Long-range PCR and mitochondrial DNA copy number quantitative PCR

Detailed methods are described in the supplementary material. The sequences of all primers used for this study are detailed in table e-1, links.lww.com/NXG/A85.

SDS-PAGE and immunoblotting

Mitochondria (25 μg) isolated from control and patient fibroblasts were separated on 4%–12% Bis-Tris gels (Invitrogen) and transferred onto a polyvinylidene difluoride (PVDF) membrane (Bio-Rad). All antibodies used are detailed in the supplementary information.

Mitochondrial protein synthesis

De novo mitochondrial protein synthesis was analyzed in fibroblasts using ^{35}S-radiolabeling of mitochondrially encoded proteins in the presence of emetine as previously described.[9] The cells were suspended in phosphate-buffered saline (PBS) and 20 μg of protein was resolved on a 12.5% SDS-PAGE gel, and radiolabelled proteins were visualized on film.

Respiration

Respiration was measured in fibroblasts as previously described.[10] The full methods are detailed in supplementary information.

Cell function measurements

JC-1, mitochondrial mass, dihydroethidium (DHE), and MTS assay full methods are detailed in supplementary information.

Statistical analysis

All data are reported as mean ± SEM. Statistical differences were determined using a two-tailed Student *t* test. JC-1, DHE, mitochondrial mass, and MTS data are expressed as a percent of average control fibroblast values for the respective media treatment.

Data availability

Study data for the primary analyses presented in this report are available upon reasonable request from the corresponding and senior author.

Results

Clinical characteristics of the patient

A 30-year-old right-handed Caucasian woman (V:2) was born to healthy consanguineous parents aged 55 and 59 years (figure 1A). There was no significant family history, and she denied a history of other diseases or past drug use. The clinical presentations were consistent with PD. Symptoms developed rapidly at age 26 years including resting tremor mostly affecting her left arm and bradykinesia. Neurologic examination at age 28 years showed general bradykinesia, rigidity, resting tremor in both hands and legs, but most prominent in the left side, with superimposed action-induced myoclonus. She also showed hypomimic face and mydriatic pupils with sluggish reaction to the light, indicating autonomic dysfunction. There were no pyramidal or cerebellar signs. On fundoscopic examination, Kayser-Fleischer-like rings were negative. Neither sphincter dysfunction nor orthostatic hypotension was present. Laboratory evaluation including thyroid function, liver function, serum and urine copper, and ceruloplasmin was unremarkable. Brain MRI was also unremarkable. The patient showed several clinical features of mitochondrial dysfunction, such as neuropsychological disturbance, dysautonomia, and myoclonus. Low-dose levodopa was started with dramatic response, but after 1 month, she had severe dyskinesia, and after 3 months, motor fluctuation, anxiety, and insomnia became the main issues and she had dopamine dysregulation syndrome. After 6 months, psychiatric problems, including aggression, depression, and impulsiveness, were additional symptoms. At follow-up at age 30 years, PD symptoms had not progressed and became stable. However, she showed signs of cognitive decline, and orthostatic hypotention added to her symptoms.

Genetic findings

Data from NGS of DNA from 1 affected (V:2) and 1 unaffected family member (V:1) were analyzed. No likely pathogenic mutations were identified in the genes included in the targeted panel of the 336 neuromuscular disease genes. WES was performed on the patient and her unaffected sister. No rare, likely pathogenic heterozygous variants in the PD-associated genes were identified. The filtering strategy of initially concentrating on homozygous coding variants in known neurogenetic disease genes, selected based on variant databases Human Genome Mutation Database and ClinVar, and the most recent literature allowed the identification of homozygous *CHCHD2* (chromosome 7) and *TOP1MT* (chromosome 8) variants. A novel homozygous missense mutation in exon 2 of *CHCHD2* (c.211G>C) (p.Ala71Pro) was identified. The size of the homozygous region covering *CHCHD2* variant on chromosome 7 was 158Mb. In addition, a homozygous missense variant of *TOP1MT* (c.661G>A, ENST00000523676, transcript ID: NM_001258447.1), changing aspartic acid to asparagine (p.Asp221Asn), was identified. No rare, likely pathogenic heterozygous or homozygous variants in the PD-associated genes, including *ATP13A2, CHCHD10, DNAJC13, EIF4G1, LRRK2, PARK2, PARK7, PARK15, PINK1, SNCA*, and *VPS35*, were identified in the exome sequencing data. The appearance of *CHCHD2* and *TOP1MT* variants was examined in available family members by sequencing analysis. Sanger sequencing confirmed segregation of both variants compatible with a recessive pattern of inheritance. The unaffected parents (IV:1, IV:2) were both heterozygous for the *CHCHD2* variant, and the healthy sister (V:1) was not a carrier (figure 1B). Both parents and the sister were heterozygous carriers of the *TOP1MT* variant (figure 1C). The c.211G>C, (p.Ala71Pro) (*CHCHD2*) variant was excluded in East and South Asian, European, African, Latino, and Ashkenazi Jewish Allele Frequency Communities (AFC), in the ExAC database, the Genome Aggregation Database (gnomAD), and the 1000 Genome database. The *TOP1MT* variant (c.661G>A, p.Asp221Asn, *rs*143769145) was a rare heterozygous variant reported in the AFC (frequency 0.025%), the ExAC (frequency 0.026%), and in the gnomAD (frequency 0.023%) databases; the variant was identified in the homozygous state. *In silico* combined annotation dependent depletion (CADD) analysis of the missense variants revealed high deleterious scores (*CHCHD2* [p.Ala71Pro]: 32.000 and TOP1MT [p.Asp221Asn]: 26.000). *In silico* analysis predicted both *CHCHD2* and *TOP1MT* substitutions to be potentially disease causing (MutationTaster, mutationtaster.org/). The 2 amino acid residues affected are highly conserved across species (figure 1D). The CHCHD2-substituted residue is located within the central conserved hydrophobic domain, the transmembrane element of the CHCHD2 protein (figure 1E). In addition, the entire coding sequence of *CHCHD2* was analyzed in 2 affected individuals of 2 large families with familial early-onset PD of Iranian origin. The *CHCHD2* p.Ala71Pro substitution was not identified, and we did not detect any other variant in this gene.

Clinical status of confirmed carriers

Cosegregation studies confirmed that the parents were carriers of *CHCHD2* and *TOP1MT* variants, and the unaffected sister was heterozygous for the *TOP1MT* variant. Given that the previously reported *CHCHD2* variants are mostly associated with late-onset dominant PD, carrier parents were examined by a neurologist. They showed no evidence of neurologic or movement disorder by history. However, the parents are still younger than the average age of PD onset (<60).[11]

Figure 1 Pedigree and genetic findings

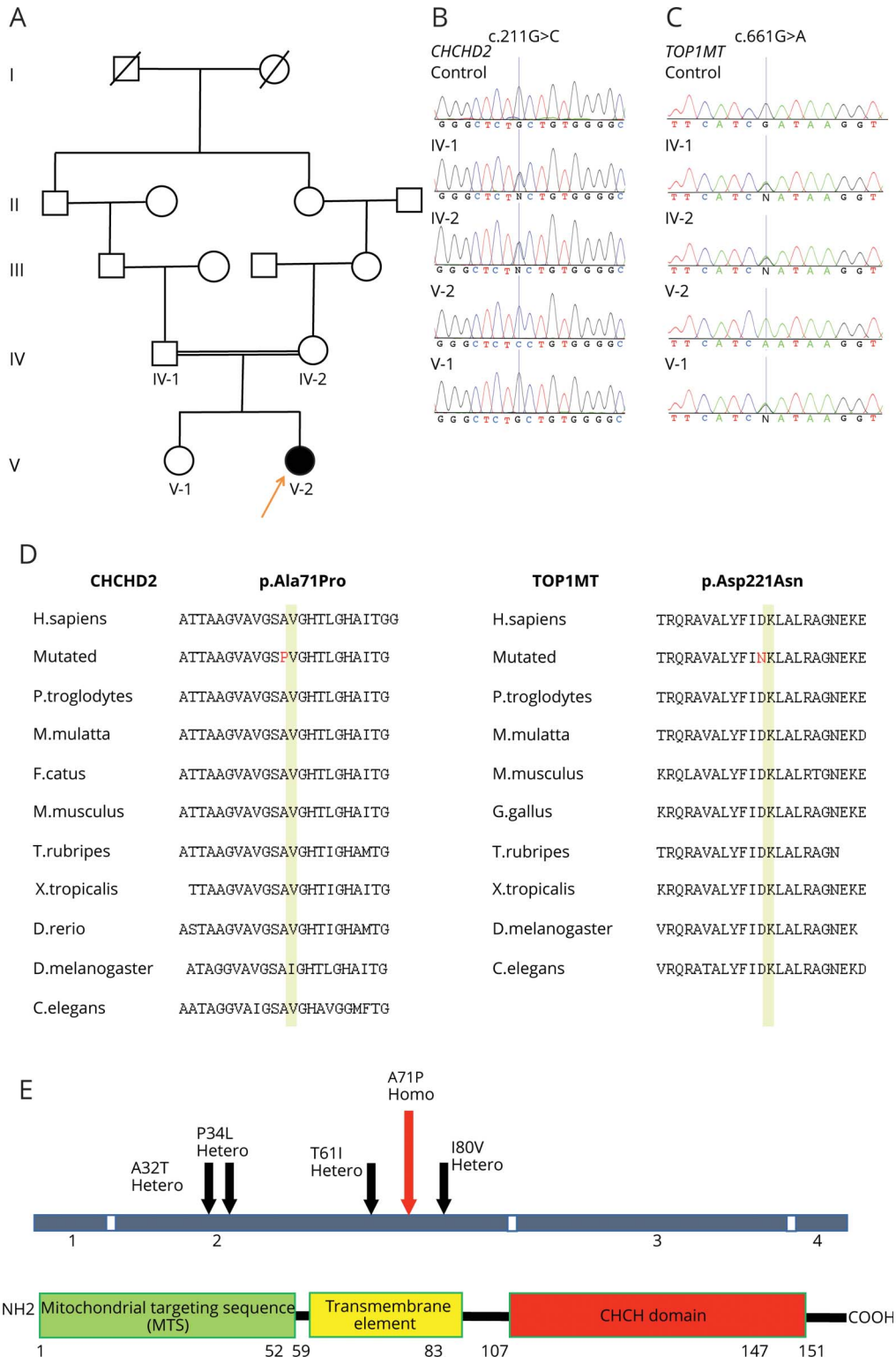

(A) Pedigree of the family. The affected individual (V:2) is represented with a shaded symbol. (B) Sanger sequence analysis demonstrates the presence of homozygous variants in *CHCHD2* and (C) *TOP1MT* in the patient and the segregation of the variants. (D) Multiple sequence alignment confirms that the p.Ala71Pro (*CHCHD2*) and p.Asp221Asn (*TOP1MT*) substitutions affect evolutionarily conserved residues (shaded). (E) Mutated residues and CHCHD2 protein structure: previously identified heterozygous missense variants associated with familial PD (black arrows) and the currently identified homozygous variant (red arrow) are all located in exon 2. The CHCHD2 p.Ala71Pro amino acid substitution is located within the central conserved hydrophobic domain at the transmembrane element.

Reduction of CHCHD2 but not TOP1MT causes the PD pathology

To investigate the molecular mechanisms behind this form of early-onset PD, dermal fibroblasts were established from the patient and compared with controls established from a healthy individual. We investigated the protein abundance by immunoblotting in patient and control fibroblasts to determine which variant was pathogenic. We observed a small reduction in TOP1MT levels, whereas the CHCHD2 reduction was more pronounced (figure 2A). As TOP1MT is the topoisomerase that catalyzes supercolied mtDNA relaxation,[12] we investigated mtDNA stability and abundance. Long-range PCR showed no mtDNA fragmentation and changes in mtDNA size in patient cells (figure 2B). Furthermore, qPCR analysis showed no significant difference in mtDNA copy number, indicating that the *TOP1MT* variant has negligible effects on mtDNA structure (figure 2, B and C).

CHCHD2 has been shown to regulate mitochondrial morphology in *Drosophila melanogaster*.[13] Therefore, we investigated mitochondrial morphology in patient cells using MitoTracker Orange. In glucose medium, we identified differences in morphology and fusion between patient and control cells, characterized by a reduced reticular network, fragmentation of filamentous mitochondria, and accumulation of granular bodies around the nucleus (figure 2D). We cultured both fibroblasts in galactose medium that stimulates a dependence on aerobic metabolism compared with cells grown in glucose media, which can rely on anaerobic metabolism. Growth in galactose exacerbated differences in mitochondrial morphology seen in patient cells (figure 2D). Our experiments excluded the mtDNA abnormalities that would be linked to TOP1MT dysfunction and identified changes in mitochondrial morphology that is related to the proposed function and membrane association identified for CHCHD2 as summarized in figure e-1, links.lww.com/NXG/A85.

The role of other CHCHD family proteins in the mitochondrial contact site and cristae organizing system (MICOS) complex[14,15] lead us to investigate how reduced CHCHD2 expression affects MICOS complex subunits. Although levels of the intermembrane protein CHCHD3 were reduced in patient cells, levels of the lipid binding proteins APOO and APOOL were unchanged (figure 2E). We conclude that although CHCHD2 does not have a direct role in MICOS complex function or stability, the CHCHD2 variant results in reduction of the membrane-associated protein CHCHD3.

Reduced CHCHD2 expression results in OXPHOS dysfunction

Impaired oxidative phosphorylation (OXPHOS) complex formation and function has been identified in PD and

Figure 2 CHCHD2 but not TOP1MT contributes to PD pathogenesis

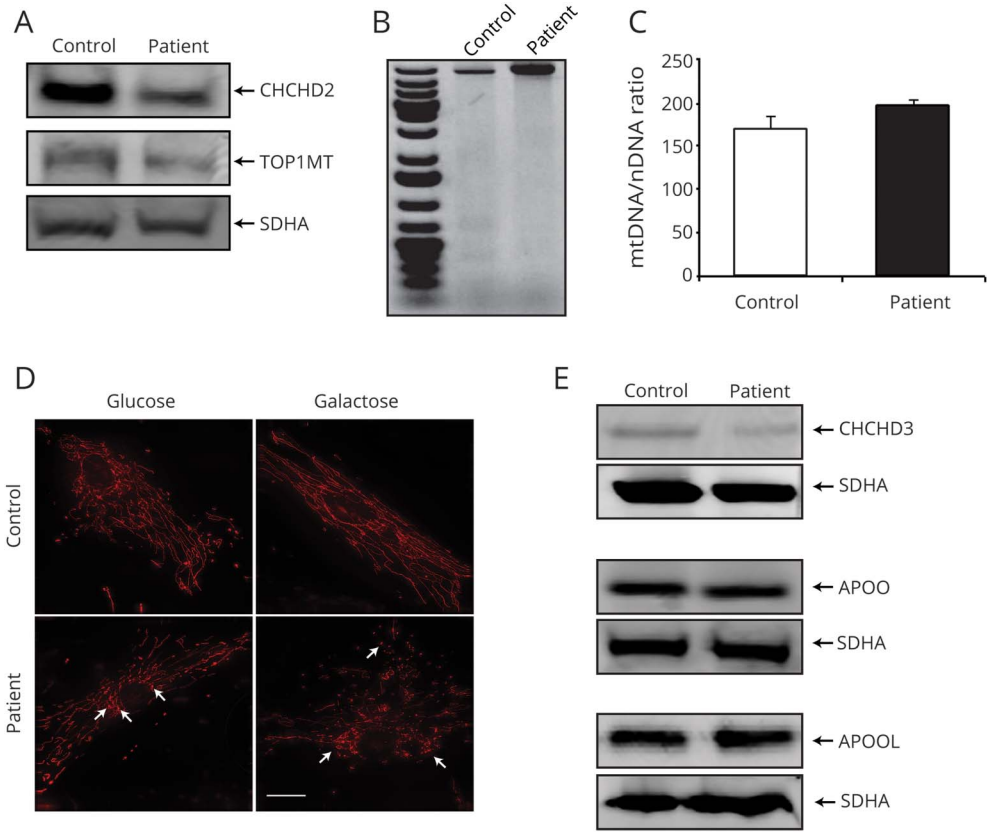

(A) SDS-PAGE and immunoblotting were performed on 25 μg of isolated mitochondria from control and patient fibroblasts. (B) Mitochondrial DNA integrity was examined using long-range PCR of control and patient fibroblast DNA. DNA was separated on a 1% agarose gel stained with ethidium bromide. (C) Mitochondrial DNA copy number was examined using quantitative PCR of control and fibroblast DNA. (D) Mitochondrial morphology of control and patient fibroblasts grown in either high glucose or galactose media was examined using MitoTracker Orange and visualized by fluorescence microscopy. The scale bar represents 10 μm. Arrows indicate refractile granules characteristic of network fragmentation. (E) Twenty-five micrograms of isolated mitochondria from control and patient fibroblasts was analyzed for mitochondrial contact site and cristae organizing system (MICOS) protein levels by immunoblotting. SDHA was used as a loading control.

drug-induced parkinsonism.[16] Therefore, we investigated OXPHOS complex subunit levels by immunoblotting. We found reduced levels of complex I, IV, and V subunits, whereas complexes II and III showed negligible reductions in patient cells (figure 3A). De novo mitochondrial translation examined using ^{35}S-methionine showed no difference in mitochondrial translation rates between control and patient cells (figure 3B). This indicates that the *CHCHD2* mutation causes changes in OXPHOS subunit abundance through reduced protein stability and morphologic changes, not impaired protein synthesis.

Next, we investigated ETC activity by measuring mitochondrial respiration at each complex (figure 3C). We show reduced oxygen consumption at complexes I and IV but not complexes II and III, suggesting that CHCHD2 may regulate electron transfer between these complexes, as previously suggested.[13,17] We also examined the respiratory control ratio (RCR) by measuring oxygen consumption with succinate and rotenone under ATP-generating conditions (phosphorylating state 3) and non-ATP generating conditions (non-phosphorylating state 4). We identified significant decreases in the RCR in patient cells grown in glucose and galactose, which is characteristic of an uncoupling of the ETC and ATP production (figure 3D). This indicates that reductions in OXPHOS activity are likely due to impaired mitochondrial morphology and electron transport between complexes.

To test whether CHCHD2 dysfunction resulted in PD, we performed rescue experiments by expressing the wild-type CHCHD2 or TOP1MT proteins in the control and patient cells (figure 4). The fragmented mitochondrial network was restored to filamentous, reticular appearance (figure 4A), and respiration was restored to levels comparable to the control fibroblast when rescued by expression of the wild-type CHCHD2 protein, but not by expression of the wild-type TOP1MT protein (figure 4B). These experiments validated the causative role of the *CHCHD2* mutation in PD pathology.

Mutation in CHCHD2 causes increased oxidative stress

Next, we investigated the mitochondrial membrane potential ($\Delta\psi_m$) using JC-1. There were no significant changes in the $\Delta\psi_m$ in patient cells grown in glucose or galactose, indicating that the proton motive force maintains the $\Delta\psi_m$ (figure 5A). The decrease in membrane potential was greater in patient cells treated with FCCP, indicating a reduction in maximal

Figure 3 Patient cells show impaired OXPHOS complex levels and function

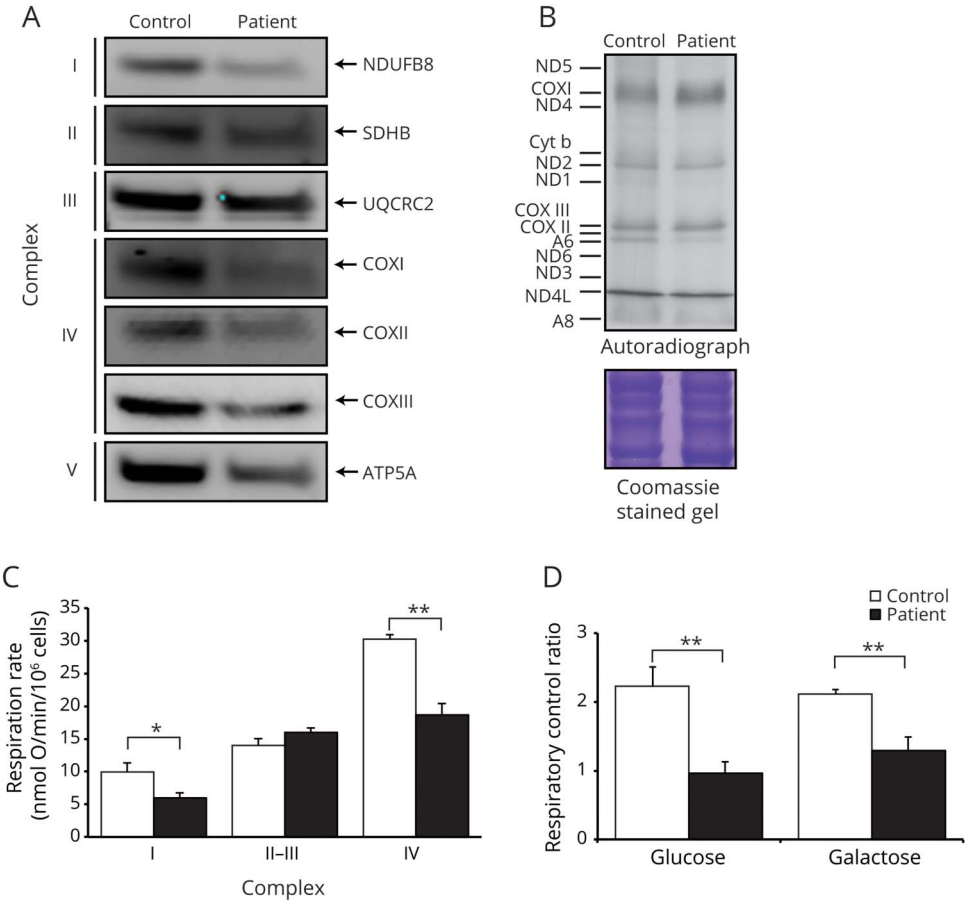

(A) SDS-PAGE and immunoblotting were performed on 25 μg of isolated mitochondria from control and patient fibroblasts. (B) Mitochondrial protein synthesis was examined in control and patient fibroblasts using ^{35}S radiolabeling of mitochondrial translation products. Twenty micrograms of cell lysate was separated on a 12.5% SDS-PAGE gel and visualized by autoradiography. (C) Oxygen consumption of specific respiratory complexes was measured in control and patient fibroblasts using an OROBOROS respirometer. (D) Phosphorylated (state 3) and non-phosphorylated (state 4) respiration was measured in the presence of 10 mM succinate/0.5 μM rotenone in digitonin-permeabilized control and patient cells to determine the respiratory control ratio under both glucose and galactose media conditions. Data are presented as mean ± SEM and were analyzed using a Student's *t* test. **p* < 0.05, ***p* < 0.01.

Figure 4 CHCHD2 but not TOP1MT expression rescues molecular defects

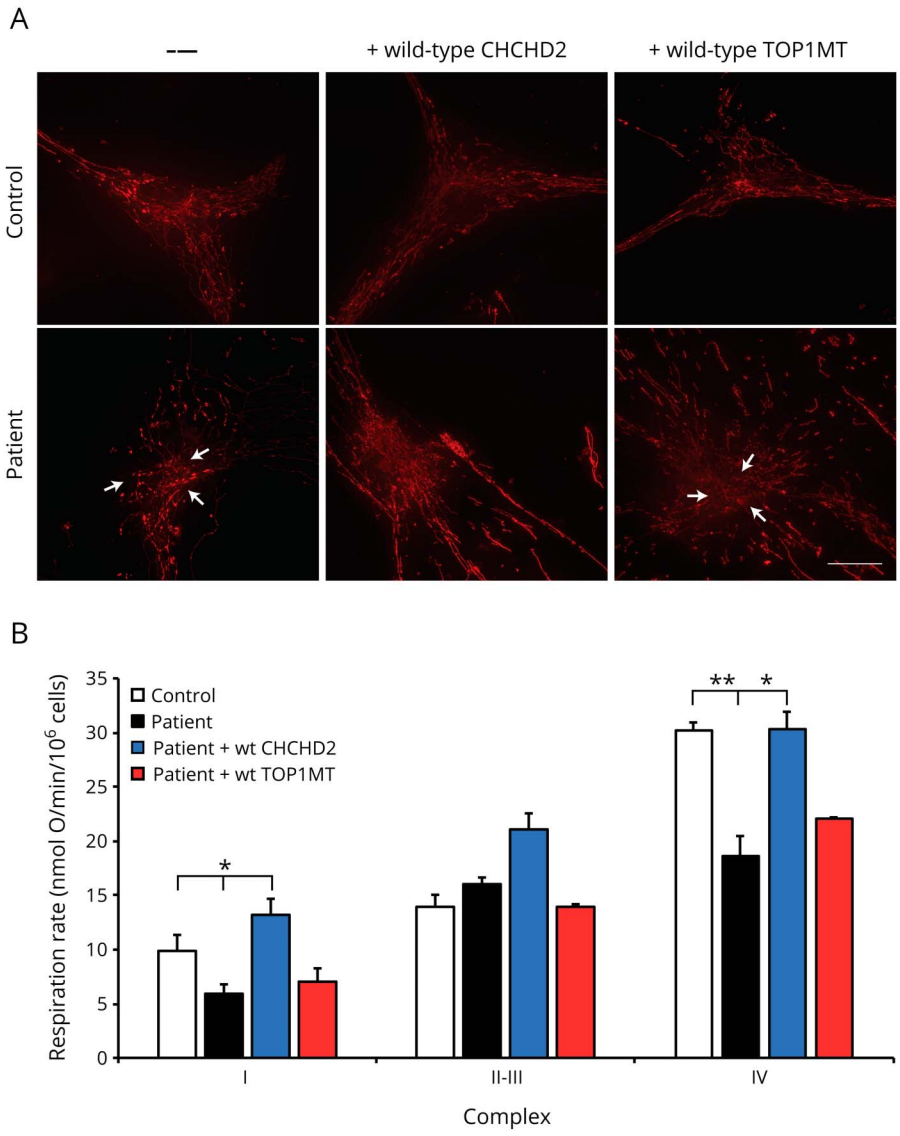

(A) Mitochondrial morphology of control and patient fibroblasts, in the presence or absence of either wild-type CHCHD2 or wild-type TOP1MT, was examined using MitoTracker Orange and visualized by fluorescence microscopy. The scale bar represents 10 μm. Arrows indicate refractile granules characteristic of network fragmentation. (B) Oxygen consumption of respiratory complexes was measured in control, patient fibroblasts, and patient fibroblasts expressing either wild-type CHCHD2 or wild-type TOP1MT using an OROBOROS respirometer. Data are presented as mean ± SEM and were analyzed using a Student's *t* test. **p* < 0.05, ***p* < 0.01.

respiratory capacity. This reduction was greater under galactose conditions (figure 5, A and B). The reduced stability of OXPHOS subunits and decreased respiratory capacity were independent of mitochondrial mass (figure 5C).

Next, we investigated reactive oxygen species (ROS) production.[18] Patient cells showed significantly increased superoxide levels when grown in glucose, which was further exacerbated when cells were grown in galactose (figure 5D). As ROS have been shown to affect metabolic rate and viability, we investigated the metabolic consequences of increased ROS levels. Patient cells showed a mild metabolic increase under glucose conditions and a further increase under galactose conditions, indicating that the increase in ROS is not inherently cytotoxic, but is sufficient to modulate the metabolic rate in skin fibroblasts (figure 5E).

Discussion

Here, we have identified homozygous *CHCHD2* and *TOP1MT* variants in a Caucasian woman presenting with characteristic features of PD at 26 years. Both healthy parents were heterozygous *CHCHD2* and *TOP1MT* variant carriers, but not the unaffected sister. The likely pathogenicity of the variants was supported by the results of the prediction tools PolyPhen-2, SIFT, and CADD, where the *TOP1MT* variant (c.661G>A, p.Asp221Asn, *rs*143769145) was identified at a low frequency of 0.023%–0.025% in the Genome Aggregation Databases with no homozygotes. The mutated residues of both CHCHD2 and TOP1MT are highly conserved during evolution. Taken together, our finding suggests that both *CHCHD2* and *TOP1MT* might be causative genes of recessive early-onset PD. Mitochondrial dysfunction has been shown to be a key factor in PD pathogenesis in both animal models and patients, with disease-associated genes

Figure 5 Patient cells demonstrate increased oxidative stress

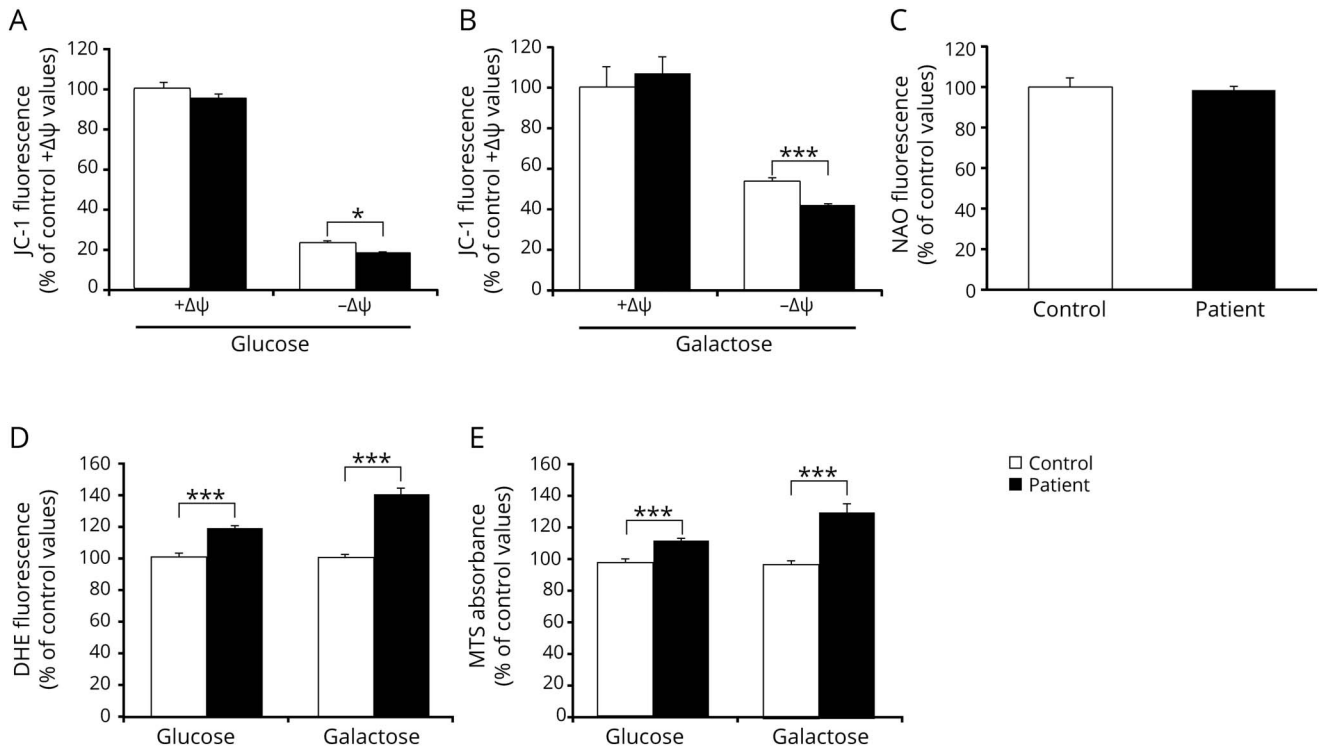

(A) JC-1 assay was used to examine the strength of the proton motive force in both control and patient fibroblasts under high glucose (A) and galactose (B) media conditions both in the absence of FCCP (+$\Delta\psi_m$) and the presence of FCCP (−$\Delta\psi_m$) (n = 6). (C) Mitochondrial mass was measured in control and patient fibroblasts using nonyl acridine orange (NAO) under high glucose conditions (n = 6). (D) Reactive oxygen species (ROS) levels were measured in control and patient fibroblasts using dihydroethidium (DHE) under both high glucose and galactose media conditions (n = 6). (E) Metabolic activity was measured in control and patient fibroblasts using an MTS assay (n = 6). All data are presented as mean ± SEM and were analyzed using a Student's *t* test. *$p < 0.05$, ***$p < 0.001$.

PINK1 and *CHCHD2* being involved in mitochondrial function.[13,19–21] Recently, however, the association of *CHCHD2* with PD has displayed mixed results in different populations,[6,7,19,22–25] suggesting that it is infrequent and ethnic specific. Here, we have used cultured patient fibroblasts to establish the pathogenic mechanisms of the identified *CHCHD2* and *TOP1MT* variants and expand the repertoire of genes implicated in the pathology of PD.

Homozygous variants of both *CHCHD2* and *TOP1MT* affected protein levels, albeit more pronounced for CHCHD2. In patient fibroblasts, the reduced CHCHD2 expression caused mitochondrial network fragmentation when cells were forced to rely on oxidative phosphorylation. This is consistent with previous studies that implicated CHCHD2 in mitochondrial morphology and its importance for energy production.[13,26] The morphology and respiration defects in the patient fibroblasts were rescued by expressing wild-type CHCHD2, providing evidence that the *CHCHD2* mutation contributes to the PD pathology. Reduced TOP1MT expression causes increased negative supercoiling of mtDNA, resulting in reduced mtDNA replication.[26] However, the lack of changes in mtDNA integrity or copy number in patient fibroblasts indicated that the *TOP1MT* variant had a negligible effect on TOP1MT function. Furthermore, the contribution of the *TOP1MT* variant to the PD pathogenesis was excluded because expression of this protein did not rescue mitochondrial morphology and function.

Changes in mitochondrial morphology have been previously linked with PD-characteristic OXPHOS deficiencies.[16,20,21,27,28] Reductions in complexes I and IV subunits were consistent with reduced activities of these complexes in patient cells. Although reduced complex IV activity has been previously reported in PD, there is much less evidence for impaired complex IV activity, contributing to PD development.[27] The reduction in complex IV formation is consistent with studies finding an interaction between CHCHD2 and the cytochrome c–binding protein MICS1.[13,29] The reduction in complex activity and function was consistent with changes in the mitochondrial membrane and indicated an uncoupling of the ETC and impaired electron transfer through the ETC,[30,31] as seen previously.[17] It is possible that reduced CHCHD2 expression causes impaired MICS1 function, therefore impairing movement of electrons from complex III to IV by cytochrome c, as previously suggested.[17]

The $\Delta\psi_m$ was not significantly altered in patient fibroblasts despite inefficient electron transfer and reduced respiratory capacity. The greater difference in uncoupled state shown under galactose conditions indicates that when patient cells are made to rely on aerobic energy sources, they can

compensate for abnormalities in ETC coupling and the electron leak through increasing the electrons flowing through the OXPHOS complexes. Although increasing electron flow may allow cells to maintain the proton motive force, it has negative consequences through ROS formation.

The increased ROS levels were not cytotoxic and, in contrast, patient fibroblasts demonstrated increased metabolic rate. Although mild increases in ROS levels have been shown to increase metabolic rate and proliferation in certain cells, such as fibroblasts, neuronal cells show reduced viability.[32–35] The mitochondrial toxicity of oxidized dopamine derivatives, in combination with the inherently low mitochondrial mass of DA neurons, may potentiate mitochondrial dysfunction resulting from reduced CHCHD2 expression and cause neuronal cell death.[33] As dermal fibroblasts may not fully emulate the characteristics of DA neurons, further investigation is needed to understand how increased ROS levels alter metabolic function in DA neurons and how they potentiate mitochondrial dysfunction resulting from reduced CHCHD2 expression.

Recent findings demonstrate that mutations in *CHCHD2* and its paralogue *CHCHD10* are associated with multiple neurodegenerative disorders.[25,36–38] The existence of a complex containing CHCHD2 and CHCHD10 may explain shared features between disorders.[39,40] In addition, CHCHD10 knockdown and knockout models show altered respiratory activity and OXPHOS subunit levels.[39,40] Further investigation is required to fully understand how this complex regulates mitochondrial and neurologic functions.

Author contributions

A. Filipovska and H. Tajsharghi: study concept and design. R.G. Lee, M. Sedghi, M. Salari, A.-M.J. Shearwood, M. Stentenbach, A. Kariminejad, H. Goullee, and O. Rackham: acquisition of data. R.G. Lee, M. Sedghi, M. Salari, A.-M.J. Shearwood, M. Stentenbach, A. Kariminejad, H. Goullee, O. Rackham, H. Tajsharghi, and A. Filipovska: analysis and interpretation. R.G. Lee, A.-M.J. Shearwood, H Goullee, and H. Tajsharghi: statistical analysis. R.G. Lee, O. Rackham, N.G. Laing, H. Tajsharghi, and A. Filipovska: critical revision of the manuscript for important intellectual content. O. Rackham, N.G. Laing, H. Tajsharghi, and A. Filipovska: study supervision.

Acknowledgment

The authors thank the family members who provided samples and clinical information for this study. The authors thank Dr Maryam Gholami for obtaining skin biopsy.

Study funding

The study was supported by grants from the European Union's Seventh Framework Programme for research, technological development and demonstration under grant agreement no. 608473 (H. Tajsharghi) and the Swedish Research Council (H. Tajsharghi). N.G. Laing is supported by NHMRC Principal Research Fellowship (APP1117510), H. Goullee by NHMRC EU Collaborative Grant APP1055295, O. Rackham by a Cancer Council WA Research Fellowship, and A. Filipovska is supported by NHMRC Senior Research Fellowship (APP1005030) and NHMRC and Australian Research Council Discovery projects (to A. Filipovska and O. Rackham). The funders had no role in the design of the study and collection, analysis, decision to publish, interpretation of data, or preparation of the manuscript.

Disclosure

R.G. Lee, M. Sedghi, M. Salari, A.-M.J. Shearwood, M. Stentenbach, A. Kariminejad, H. Goullee, and O. Rackham report no disclosures. N.G. Laing has received a speaker honorarium from the World Muscle Society; has received travel funding from the Asian Oceanian Myology Centre, Sanofi, and the Ottawa Neuromuscular Meeting; serves on the editorial board of *Neuromuscular Disorders*; receives publishing royalties for The Sarcomere and Skeletal Muscle Disease, Springer Science and Business Media, Landes Bioscience, 2008; and has received research support from the Australian National Health and Medical Research Council, the US Muscular Dystrophy Association, Association Francaise contre les Myopathies, Foundation Building Strength for Nemaline Myopathy, Motor Neuron Disease Research Institute of Australia, Western Australian Health and Medical Research Infrastructure Fund, and the Perpetual Foundation. H. Tajsharghi and A. Filipovska report no disclosures. Full disclosure form information provided by the authors is available with the full text of this article at Neurology.org/NG.

Received February 28, 2018. Accepted in final form June 18, 2018.

References

1. Liu G, Bao X, Jiang Y, et al. Identifying the association between Alzheimer's disease and Parkinson's disease using genome-wide association studies and protein-protein interaction network. Mol Neurobiol 2015;52:1629–1636.
2. Mhyre TR, Boyd JT, Hamill RW, Maguire-Zeiss KA. Parkinson's disease. Subcell Biochem 2012;65:389–455.
3. Thomas B, Beal MF. Parkinson's disease. Hum Mol Genet 2007;16:R183–R194.
4. Lill CM. Genetics of Parkinson's disease. Mol Cell Probes 2016;30:386–396.
5. Funayama M, Ohe K, Amo T, et al. CHCHD2 mutations in autosomal dominant late-onset Parkinson's disease: a genome-wide linkage and sequencing study. Lancet Neurol 2015;14:274–282.
6. Shi CH, Mao CY, Zhang SY, et al. CHCHD2 gene mutations in familial and sporadic Parkinson's disease. Neurobiol Aging 2016;38:217.e9–217.e13.
7. Jansen IE, Bras JM, Lesage S, et al. CHCHD2 and Parkinson's disease. Lancet Neurol 2015;14:678–679.
8. Rackham O, Davies SMK, Shearwood AMJ, Hamilton KL, Whelan J, Filipovska A. Pentatricopeptide repeat domain protein 1 lowers the levels of mitochondrial leucine tRNAs in cells. Nucleic Acids Res 2009;37:5859–5867.
9. Davies SMK, Rackham O, Shearwood AMJ, et al. Pentatricopeptide repeat domain protein 3 associates with the mitochondrial small ribosomal subunit and regulates translation. FEBS Lett 2009;583:1853–1858.
10. Sanchez MIGL, Mercer TR, Davies SMK, et al. RNA processing in human mitochondria. Cell Cycle Georget Tex 2011;10:2904–2916.
11. Lesage S, Brice A. Parkinson's disease: from monogenic forms to genetic susceptibility factors. Hum Mol Genet 2009;18:R48–R59.
12. Zhang H, Zhang YW, Yasukawa T, Dalla Rosa I, Khiati S, Pommier Y. Increased negative supercoiling of mtDNA in TOP1mt knockout mice and presence of topoisomerases IIα and IIβ in vertebrate mitochondria. Nucleic Acids Res 2014;42:7259–7267.
13. Meng H, Yamashita C, Shiba-Fukushima K, et al. Loss of Parkinson's disease-associated protein CHCHD2 affects mitochondrial crista structure and destabilizes cytochrome c. Nat Commun 2017;8:15500.
14. Ding C, Wu Z, Huang L, et al. Mitofilin and CHCHD6 physically interact with Sam50 to sustain cristae structure. Sci Rep 2015;5:16064.

15. Li H, Ruan Y, Zhang K, et al. Mic60/Mitofilin determines MICOS assembly essential for mitochondrial dynamics and mtDNA nucleoid organization. Cell Death Differ 2016;23:380–392.
16. Richardson JR, Caudle WM, Guillot TS, et al. Obligatory role for complex I inhibition in the dopaminergic neurotoxicity of 1-methyl-4-phenyl-1,2,3,6-tetrahydropyridine (MPTP). Toxicol Sci 2007;95:196–204.
17. Aras S, Bai M, Lee I, Springett R, Hüttemann M, Grossman LI. MNRR1 (formerly CHCHD2) is a bi-organellar regulator of mitochondrial metabolism. Mitochondrion 2015;20:43–51.
18. Murphy MP. How mitochondria produce reactive oxygen species. Biochem J 2009; 417:1.
19. Liu Z, Guo J, Li K, et al. Mutation analysis of CHCHD2 gene in Chinese familial Parkinson's disease. Neurobiol Aging 2015;36:3117.e7–3117.e8.
20. Morais VA, Haddad D, Craessaerts K, et al. PINK1 loss-of-function mutations affect mitochondrial complex I activity via NdufA10 ubiquinone uncoupling. Science 2014; 344:203–207.
21. Morais VA, Verstreken P, Roethig A, et al. Parkinson's disease mutations in PINK1 result in decreased Complex I activity and deficient synaptic function. EMBO Mol Med 2009;1:99–111.
22. Liu G, Li K. CHCHD2 and Parkinson's disease. Lancet Neurol 2015;14:679–680.
23. Foo JN, Liu J, Tan E-K. CHCHD2 and Parkinson's disease. Lancet Neurol 2015;14: 681–682.
24. Iqbal Z, Toft M. CHCHD2 and Parkinson's disease. Lancet Neurol 2015;14: 680–681.
25. Rubino E, Brusa L, Zhang M, et al. Genetic analysis of CHCHD2 and CHCHD10 in Italian patients with Parkinson's disease. Neurobiol Aging 2017; 53:193.e7–193.e8.
26. Rambold AS, Kostelecky B, Elia N, Lippincott-Schwartz J. Tubular network formation protects mitochondria from autophagosomal degradation during nutrient starvation. Proc Natl Acad Sci USA 2011;108:10190–10195.
27. Benecke R, Strümper P, Weiss H. Electron transfer complexes I and IV of platelets are abnormal in Parkinson's disease but normal in Parkinson-plus syndromes. Brain J Neurol 1993;116(pt 6):1451–1463.
28. JasonCannon R, Tapias VM, Na HM, Honick AS, Drolet RE, Greenamyre JT. A highly reproducible rotenone model of Parkinson's disease. Neurobiol Dis 2009;34:279–290.
29. Oka T, Sayano T, Tamai S, et al. Identification of a novel protein MICS1 that is involved in maintenance of mitochondrial morphology and apoptotic release of cytochrome c. Mol Biol Cell 2008;19:2597–2608.
30. Brand MD, Nicholls DG. Assessing mitochondrial dysfunction in cells. Biochem J 2011;435:297–312.
31. Jastroch M, Divakaruni AS, Mookerjee S, Treberg JR, Brand MD. Mitochondrial proton and electron leaks. Essays Biochem 2010;47:53–67.
32. Hwang O. Role of oxidative stress in Parkinson's disease. Exp Neurobiol 2013;22: 11–17.
33. Valencia A, Morán J. Reactive oxygen species induce different cell death mechanisms in cultured neurons. Free Radic Biol Med 2004;36:1112–1125.
34. Emdadul Haque M, Asanuma M, Higashi Y, Miyazaki I, Tanaka K, Ogawa N. Apoptosis-inducing neurotoxicity of dopamine and its metabolites via reactive quinone generation in neuroblastoma cells. Biochim Biophys Acta 2003;1619:39–52.
35. Liang CL, Wang TT, Luby-Phelps K, German DC. Mitochondria mass is low in mouse substantia nigra dopamine neurons: implications for Parkinson's disease. Exp Neurol 2007;203:370–380.
36. Bannwarth S, Ait-El-Mkadem S, Chaussenot A, et al. A mitochondrial origin for frontotemporal dementia and amyotrophic lateral sclerosis through CHCHD10 involvement. Brain J Neurol 2014;137:2329–2345.
37. Johnson JO, Glynn SM, Gibbs JR, et al. Mutations in the CHCHD10 gene are a common cause of familial amyotrophic lateral sclerosis. Brain J Neurol 2014;137:e311.
38. Müller K, Andersen PM, Hübers A, et al. Two novel mutations in conserved codons indicate that CHCHD10 is a gene associated with motor neuron disease. Brain J Neurol 2014;137:e309.
39. Straub IR, Janer A, Weraarpachai W, et al. Loss of CHCHD10–CHCHD2 complexes required for respiration underlies the pathogenicity of a CHCHD10 mutation in ALS. Hum Mol Genet 2018;27:178–189.
40. Burstein SR, Valsecchi F, Kawamata H, et al. In vitro and in vivo studies of the ALS-FTLD protein CHCHD10 reveal novel mitochondrial topology and protein interactions. Hum Mol Genet 2018;27:160–177.